Organic matter sources for tidal marsh sediment over the past two millennia in the Minho River estuary (NW Iberian Peninsula).

J.M. De la Rosa [a*], M.F. Araújo [b], J.A. González-Pérez [a], F.J. González-Vila [a], A.M. Soares [b], J.M. Martins [b, c], E. Leorri [d], R. Corbett [d], F. Fatela [e]

[a] *Instituto de Recursos Naturales y Agrobiología de Sevilla (IRNAS-CSIC). Av. Reina Mercedes 10, 41012, Seville, Spain*

[b] *Instituto Superior Técnico-Instituto Tecnológico e Nuclear. Estrada Nacional 10, 2686-953, Sacavém, Portugal*

[c] *Universidade do Algarve, Faculdade de Ciências e Tecnologia, Campus de Gambelas, 8005-139 Faro, Portugal*

[d] *Geological Sciences, East Carolina University. 101 Graham building, Greenville, NC 27858-4353, USA*

[e] *Universidade de Lisboa. Faculdade de Ciências, Centro e Departamento de Geologia, Campo Grande, 1749-016 Lisbon, Portugal*

[*]Corresponding author. Tel. +351-219946221; fax: +351-219946185.

E-mail address: jmrosa@irnase.csic.es (Jose M. De la Rosa).

ABSTRACT

Environmental changes during the last 2 millennia in the Minho River tidal marsh (NW Portugal-Spain border) were reconstructed. Changes in the sources of organic matter (OM) delivered to the marsh were evaluated from elemental, isotopic and molecular composition using a 1 m sediment core. Carbon isotopic composition ($\delta^{13}C$) and organic carbon to total nitrogen ratio (C_{org}/N) provided valuable information concerning the origin of the OM. These parameters indicated a major input from land plants, reaching a maximum at 1100–1200 and 1750–1850 AD. These periods match with major flood events in the NW of the Iberian Peninsula, as reported by several authors. A significant reduction in the terrestrial signature occurred at 6–4 cm (ca. 1960–1985 AD), which is contemporaneous with the construction of several major dams on the Minho River. The distribution of selected lipid biomarkers, including *n*-alkanes, *n*-fatty acids and *n*-alkan-2-ones and specific parameters derived from the molecular distributions, were useful for refining bulk geochemical results. Long chain *n*-alkanes with an odd number of carbons are indicators of soil-and vascular plant-derived terrestrial OM and were dominant throughout the core. In addition, a greater contribution of plankton-derived lipids was observed in the sections corresponding to ca. 1960–1985 AD (6–4 cm) and ca. 100–200 AD (96–94 cm). Although different degradation rates for individual compounds might have partly affected biomarker assemblages, the variations could be attributed to a sharp decrease in the freshwater contribution to the Minho River Estuary (dam construction) and a possible marine highstand, respectively. In addition, several parameters suggested changes in land use (including deforestation and

farming) and probably the effects of mining exploitation during the Roman occupation of the area.

Keywords: Sedimentary organic matter; Minho estuary; tidal marsh; biomarkers; $\delta^{13}C$; geochronology.

1. Introduction

Sheltered coastal environments, such as estuaries, lagoons, bays, rias and tidal marshes commonly preserve thick sequences of sediments, offering the opportunity to investigate not only global alteration, including climate change, but also more local events (Lamb et al., 2006). Such environments are key locations for organic matter (OM) burial, and play an essential role in the global carbon cycle. It is estimated that > 90% of the total organic carbon (TOC) preserved in marine sediments is buried in deposits along the estuarine areas and continental margins in "terrigenous-deltaic" regions near river mouths (Berner et al., 1989). Common to all estuarine areas is a diversity of OM sources, particularly estuarine tidal marshes and tidal flats that receive sediment from several sources, including fluvial- and marine-derived minerogenic sediment and particulate OM, as well as OM from tidal marsh plants and other biota (Meyers and Ishiwatari, 1993).

The northwest of the Iberian Peninsula exhibits most significant correlation with the North Atlantic Oscillation (NAO) in Europe. The correlation suggests that the region is a site of key importance for climate reconstruction in the North Atlantic (Abrantes et al., 2011). The main goal of this study was to reconstruct the history of OM accumulation in a tidal salt marsh in the Minho estuary. This objective is important given the strategic location of the estuary for climatic reconstruction and the lack of information regarding OM sources, transport and fate in the area.

In our study, sedimentary OM was characterized using several complementary organic geochemical methods and indices, including elemental

carbon, nitrogen and sulfur abundance (C, N, S), molar OC to nitrogen and sulfur ratios (C_{org}/N; C_{org}/S) and stable organic carbon isotope ($\delta^{13}C$) values. These parameters have been widely used to determine historical changes in sources of OM in tidal marsh sediments and coastal areas (e.g. Burdloff et al., 2008; Hedges and Oades, 1997; Perdue and Koprivnjak, 2007; Müller and Mathesius, 1999; Thornton and McManus, 1994). Typical atomic C_{org}/N values for fresh marine organisms are within a range of 4–10, much lower than those for terrestrial plants (≥ 20), which contain cellulose, lignin and tannins (Uzaki and Ishiwatari, 1986; Meyers, 1994).

The isotopic ratio of land-derived C_3 biomass ranges from –23‰ to –34‰, with an average of ca. –27‰, while typical marine end member values are –18‰, to –22‰ for $\delta^{13}C_{org}$ (Meyers, 1997; Holtvoeth et al., 2005). Bulk $\delta^{13}C_{org}$ and C_{org}/N should therefore reflect the relative amounts of the sources of OM; however, their ability to precisely identify OM sources is uncertain when decomposition processes affect the sedimentary column (Thornton and McManus, 1994). Due to the different response to diagenetic processes by C and N, the C_{org}/N ratio of terrestrial OM tends to decrease, while that of algae tends to increase (Meyers et al., 1984).

In order to overcome the above potential issues in identifying different OM sources, we also employed the distributions of several classes of lipid biomarker compounds. Lipid biomarkers have been widely used as tracers, or proxies, for characterizing the nature and distribution of OM in aquatic systems because they are often source specific (González-Vila et al., 2003; Volkman, 2006). By choosing lipid classes or specific lipids that represent different

sources of OM, it is possible to identify the relative contributions of autochthonous and allochthonous OM input to the sedimentary record over a range of temporal and spatial scales (Wakeham et al., 1991; Meyers, 2003; Rosell Melé, 2003). Among terrestrial biomarkers, straight long chain ($\geq C_{21}$) alkanes and alkanoic acids are known as major compounds derived from leaf wax. Their abundance and distribution may be used to indicate inputs of land-derived material to a system (Meyers and Ishiwatari, 1993; Ficken et al., 2002).

Using shifts in the elemental and isotopic composition as well as the lipid assemblages isolated from sections of a sediment core from the Minho River estuary, we obtained information recording the origin, dispersal pathways, and alteration and transformation of OM. The chronological framework was established using a combination of techniques (^{210}Pb, ^{137}Cs and ^{14}C).

2. Material and methods

2.1. Study area and sampling

The Minho River originates in Serra da Meira, in the province of Lugo (Spain) and drains into the Atlantic Ocean. It has a high environmental value; in fact its 310 km extent has been considered a biosphere reserve by the UNESCO since 2002. The watershed drains an area of 17080 km^2 and is dominated by granite, greywacke and schist. The river lower estuary is located on the northwest coast of the Iberian Peninsula and has a maximum width of just over 2 km. This high-mesotidal estuary is partially mixed; however, during periods of high flow, it tends to evolve towards a salt wedge estuary. The influence of spring tides extends ca. 40 km upstream. Water flow averages 340

119 $m^3 s^{-1}$, but the winter peak discharge (December to March) usually exceeds
120 1000 $m^3 s^{-1}$ and a 100 yr flood recorded 6100 $m^3 s^{-1}$ (Bettencourt et al., 2003).
121 However, the water flow has been drastically reduced during the second half of
122 the past century due to the effect of the construction of several dams (Schmidt
123 et al., 2010).

124 The lower estuary is very shallow; most of the estuary is exposed during the
125 low water spring tides as a result of widespread siltating. A large tidal flat and
126 tidal marsh surface of around 6 km^2 have developed in the margins. Previous
127 fieldwork in the Caminha tidal marsh showed this stable accumulative
128 environment to have existed for at least the last 7000 yr, exhibiting ideal
129 conditions for studying the evolution of environmental proxies preserved in its
130 sedimentary record.

131 In June 2010, several 1 m cores were collected in the estuary with a
132 manual auger corer at 41º 52' 37" N and 8º 49' 28" W (Fig. 1). After core
133 description and photographic documentation, cores were immediately
134 transported to the laboratory and carefully sliced with a ZrO_2 knife into 1 cm
135 sections for geochronology and 2 cm sections for bulk and lipid analysis.
136 Samples for lipid analysis were wrapped in solvent-cleaned Al foil until
137 extraction.
138

139 *2.2. Analytical work*

140 *2.2.1. Elemental analysis*

141 Freeze-dried samples were used for biogeochemical analyses. Total
142 carbon (TC), total nitrogen (TN) and total sulfur (TS) contents were determined

in triplicate on ground and homogenised aliquots using an elemental analyzer (Carlo-Erba EA-1110 microanalyzer). TOC content were measured after pre-treatment with 2M HCl (3 x) to remove carbonate. Total inorganic carbon (TIC) was obtained from the difference between TC and TOC (Nieuwenhuize et al., 1994). The instrumental readings were checked against aliquots of a sulphanilamide standard. The analytical error based on triplicate analyses was within 5% to 8% for TOC, TS and TN.

2.2.2. $\delta^{13}C$ measurements

Carbon (^{13}C) isotope analysis was performed on decarbonized sediments. An aliquot (ca. 1g) of each core section was ground to a fine powder, homogenized in a ball mill, treated with 2M HCl (3x), and washed and dried (40 ºC; 48 h). Analysis was carried out with an elemental analyzer interfaced to a continuous flow isotope ratio mass spectrometer (Sercon 20-20 EA-IRMS; Sercon Ltd.) on triplicate aliquots of each sample (between 1 and 5 mg) packed into tin capsules and combusted in excess oxygen at 1000 ºC in a reactor packed with chromium oxide, copper oxide and silver wool. Rsults are expressed as per mil deviation (‰) from Peedee Belemnite ($^{13}C/^{12}C$, PDB). The reproducibility of the procedure was in the range of 0.1–0.2‰.

2.2.3. Geochronology

Dating recent marsh sediments usually relies on determination (Appleby and Oldfield, 1992) of the vertical distribution of unsupported ^{210}Pb (half life 22.3 yr) Total ^{210}Pb was measured via α spectroscopy following the methodology of

Nittrouer et al. (1979). An aliquot (ca. 1.5 g) of sediment was spiked with ^{209}Po and partially digested with 8 N HNO_3 via microwave heating. ^{209}Po and ^{210}Po in solution were then electroplated onto Ni planchets in dilute acid (modified from Flynn, 1968). $^{210}Pb_{Excess}$ was determined by subtracting the ^{210}Pb activity supported by ^{226}Ra from the total ^{210}Pb activity, where the supported ^{210}Pb activity for a given core was assumed to be equal to the uniform background activity found at depth (Nittrouer et al., 1979). The simple model proposed by Robbins (1978) and a constant rate of supply (CRS; Appleby and Oldfield, 1978) were used as they are the most suitable for the region (Irabien et al., 2008; Leorri et al., 2010). Two additional samples (41 cm and 91 cm depth) were analyzed for ^{14}C at Beta Analytic Inc. (USA) to provide a complete chronological framework (Table 1). Sediments were pretreated by acid wash and subjected to accelerator mass spectrometry (AMS) ^{14}C dating. Conventional radiocarbon dates were calibrated using IntCal09 (Reimer et al., 2009).

2.2.4. Lipid extraction and analysis

Freeze-dried sediment (ca. 5 g) was ground in a mortar and free lipids were extracted using Soxhlet apparatus with CH2Cl2:MeOH (3:1, v/v; suprasolv Merck) for 16 h. Elemental S was removed from the extract using activated Cu and the extract was concentrated using a rotary evaporator. Total lipid content was determined in duplicate by gravimetry and expressed relative to TOC. An aliquot of concentrated extract was saponified (3 h, reflux with 0.5 N KOH in MeOH). Neutral and acid fractions were isolated by extraction with hexane before and after acidification to pH <1, respectively. The acid fractions was methylated (trimethylsilyldiazomethane, $TMSCHN_2$) according to Hashimoto et

al. (1981) and silylated with N,O-bis(trimethylsilyl)trifluoroacetamide (BSTFA; 50 µL, 40 °C, 40 min) before analysis using gas chromatography–mass spectrometry (GC–MS; Hewlett-Packard GCD 5730A).

Separation of acid and neutral compounds was achieved using a SE-52 fused silica column (30 m × 0.32 mm i.d., film thickness 0.25 µm). The oven temperature was programmed from 40 to 100 °C at 30 °C min^{-1} and to 300 °C at 6 °C min^{-1}. He was the carrier gas at 1 ml min^{-1}. Mass spectra were obtained over *m/z* 50 to 550at 70 eV ionizing energy. Individual compounds (*n*-alkanes, *n*-fatty acids and *n*-alkan-2-ones) were identified by displaying traces corresponding to selected ions characteristic for the homologous series (*m/z* 57, *m/z* 74 and *m/z* 58, respectively) and by comparison of mass spectra with spectra in libraries (NIST and Wiley). Most biomarker series occurred in low concentration, so absolute concentrations were subject to considerable inaccuracy. Therefore, only semi-quantitative component abundance was assessed using the SIM traces assuming constant relationship between the reconstructed ion current response and the amount of a component in the corresponding sub-fraction.

3. Climatic variation in the NW of the Iberian Peninsula during the last two millennia

Several authors have studied the deviations in the climatic conditions of the North of the Iberian Peninsula from the last phases of the Holocene until the present. For instance, Martínez-Cortizas et al. (1999) derived a record of Hg deposition in the peat bog of Penido Vello in northwest Spain, twhich extends to

4000 ^{14}C yr before the present. Desprat et al. (2003) studied the climatic variability for the last three millennia in northwest Iberia via high resolution pollen analysis of a sediment core retrieved from the central axis of the Ria de Vigo in south Galicia, whereas Pla and Catalan (2005) analysed chrysophyte cyst data for 105 lakes within the Central and Eastern Pyrenees of northeast Spain to produce a Holocene history of winter/spring temperatures. They found an alternation of cold periods with relatively warm episodes. In the order of their occurrence, the periods were described as the Late Iron Cold Period, (<150 BC), which was followed by a warmer and wetter phase, the Roman Warm Period (RWP; 150 BC–450 AD). The period between 450 and 950 AD was again cold and dry, concomitant with the Dark Ages (DAs), that terminated with the onset of the Medieval Warm Period (MWP; 950–1400 AD). The MWP was followed by a phase of high climate variability but under lower temperature, the Little Ice Age (LIA) (1400–1850 AD), which includes the Maunder Minimum (around 1670–1750 AD). The LIA was succeeded by the recent warming (1850 AD to the present). In addition, several strong flooding episodes are documented during these periods and were especially common at times of transitions between periods (e.g. 500–600, 1100–1200 and 1450–1600 AD; Abrantes et al., 2011; Benito et al 1996). During the 18th and 19th centuries, intensive precipitation and thunderstorms were common, alternating with severe droughts, as recorded in other localities from southern and northern Spain (Riera et al., 2004; Benito et al., 2008; Gil-Garcia et al., 2008; Martin-Puertas et al., 2008).

4. Results and discussion

4.1. Chronology and bulk Geochemical parameters

Downcore values for geochronology, elemental (C, N, S), carbon iδ^{13}C, lipid content and the atomic ratios C_{org}/N, C_{org}/S for the sediment sections are plotted in Fig. 2.

The core showed an exponential, although variable, decline in $^{210}Pb_{Excess}$ with depth and the plot of the natural log of ^{210}Pb was fairly linear. The pattern suggests a relatively constant rate of deposition, allowing us to use the simple model of Robbins (1978). However, an inflexion in the $^{210}Pb_{Excess}$ pattern suggests that there could have been a short term fluctuation in net deposition, so the CRS model (Appleby and Oldfield, 1978) was also used.

Leorri et al. (2010) showed a strong variability in sedimentation rate in response to environmental change, spatial distribution and human impact on the Atlantic coast of the Iberian Peninsula. At the Minho site, ^{210}Pb activity showed a general decline with depth And the profile did not suggest any major mixing or disruption in sedimentation. Estimates derived from the simple and CRS models were in agreement in the long term (100 yr) and indicate that the sediments of the uppermost 10 cm were deposited over the last 100 yr. The main difference occurred at 8 cm, where CRS indicated an inflexion in sedimentation rate, i.e. lower values at the bottom of the core. The CRS model was in better agreement with ^{137}Cs and total Pb concentration (see Leorri et al., 2008 for discussion).

The two ^{14}C dates recovered at 41 cm and 91 cm gave 1470 and 250 yr AD (intercept values), respectively. We used the full 2σ error when calculating

263 the trends: Cal AD 1440 to 1530 (Cal BP 510 to 420)/Cal AD 1560 to 1630 (Cal
264 BP 390 to 320) and Cal AD 220 to 350 (Cal BP 1730 to 1600). The derived
265 sedimentation rate rangeg from 0.5 to 1 mm yr^{-1}. The values are typical for
266 many mesotidal marshes elsewhere in NW Europe (e.g. Cundy and Croudace,
267 1995) and were supported by results derived from both ^{210}Pb and ^{14}C from
268 nearby cores (Leorri et al., 2010).

269 The TOC content varied from 14.1% to 1.9% (of total wt.). It decreased
270 significantly downcore from 0 cm to 50 cm, being consistent with the effects of
271 diagenesis, and remained relatively constant around 2% in the sections below
272 60 cm (<1000 AD). Similar trends were observed forTN content, which varied
273 from 1.30 wt.% (1960–1985 AD) to 0.12 wt.% (300–400 AD). The positive
274 correlation between TOC and TN (r^2 0.94) suggested that N was predominantly
275 fixed in the OM (Sabel et al., 2005). The atomic C_{org}/N ratio has been widely
276 used to distinguish potential OM origins. Because of the content of peptide
277 material, typical C_{org}/N values for fresh marine biogenic OM vary between 4 and
278 10, whereas OM from terrestrial vascular plants has a ratio of 20 and higher
279 because it contains cellulose, lignin and tannins (Uzaki and Ishiwatari, 1986;
280 Meyers, 1994; 1997). The C_{org}/N ratio in the core (Fig. 2) was mostly >15,
281 attributable to a predominantly terrestrial origin for the sedimentary OM, with
282 some variable contribution of marine OM. Similar values were reported for salt
283 marsh sediments (Alberts and Filip, 1989) and for recent sediments sampled
284 from several estuarine and riverine areas within the Iberian Peninsula (De la
285 Rosa et al., 2011; Polvillo et al., 2009). According to their low C_{org}/N values,
286 sections corresponding to 1960–1985 AD and 50–250 AD, pointed to a greater

287 marine contribution than the rest. However, one should be cautious with such
288 an interpretation since diagenetic processes must always be considered
289 (Lehmann et al., 2002). The low C_{org}/N values in the deepest sections of the
290 core could indicate a preferential utilization of C and bacterial immobilization of
291 N, as reported for lacustrine sediments (Meyers and Ishiwatari, 1993). Thus,
292 additional parameters were considered (see below) to confirm these
293 hypotheses.

294 TIC ranged from 1.9 to 0.1 wt.%, decreasing downcore, with the
295 exception of the section corresponding to 1500–1600 AD (46–44 cm). TS
296 values forthe upper 54 cm of (1100–2010 AD) are similar to those reported by
297 Schmidt et al (2009) for recent sediments taken in the coastal area around the
298 Minho river mouth (0.14 to 0.28%). Total S content was higher in the sections
299 corresponding to 50–1050 AD (max. 0.46%; mean 0.37$\pm$0.06%). Consequently,
300 very low C_{org}/S values occurred below 60 cm, pointing to an increase in
301 reducing conditions (Hadas et al., 2001) during sediment deposition for that
302 period (> 1000 yr ago). Nevertheless, another factor may have contributed to
303 this significant increase in TS content. The Au and Cu wealth of this Celtic
304 region motivated the Roman conquest in 25 BC. After the domination of the
305 Roman army, the northwestern Iberian Peninsula became the biggest Au
306 producer in the Roman Empire. The arsenopyrite and chalcopyrite ores of
307 Galicia were exploited during the 400 yr of Roman domination of the Iberian
308 Peninsula. Millions of m^3 of rock were moved from more than 200 open pits in
309 western Asturias, León and Galicia through elaborate hydraulic mining methods
310 using water supplied by hundreds of km of canals that traverse the mountainous

311 countryside (Sánchez-Palencia and Suárez, 1988). In this sense, it is known
312 that the transfer of larger quantities of reactive OM to anoxic zones increases
313 sulfate reduction, decreasing considerably the C_{org}/S ratio (Leventhal, 1983).
314 Nevertheless further studies would be needed to confirm this hypothesis.
315 $\delta^{13}C$ values are neither significantly influenced by sediment grain size
316 nor particularly sensitive to environmental or depositional factors, making them
317 useful indicators in reconstructing past sources of OM (Meyers, 1997). Thus the
318 isotopic difference between OC produced by C_3 land plants and marine algae
319 has been used to trace the delivery of OM to sediments of estuarine and coastal
320 areas (Prahl et al., 1994). In our core, the $\delta^{13}C$ value of TOC ranged between –
321 25.0 and –27.4‰, values typically reported for C_3 land plant biomass (Meyers,
322 1994), suggesting a dominantly terrestrial input. The sharp change at 4 cm
323 (1960–1985 AD) towards less negative values (–25.0‰) was accompanied by a
324 decrease in C_{org}/N (12.1). Both are indicative of a greater marine OM input at
325 that period. The change may be the result of a drastic decrease in the Minho
326 river discharge caused by the construction of several dams from the 1960s to
327 the 1970s (E1; Fig. 2). The $\delta^{13}C$ values zigzag in the intervals corresponding to
328 1850–1750 AD (E2; Fig. 2). This period corresponds to the end of the LIA, in
329 which intensive precipitation, snowfall and thunderstorms were common,
330 alternating with severe droughts, as recorded for other localities from southern
331 and northern Spain (Riera et al., 2004; Gil-Garcia et al., 2008; Martin-Puertas et
332 al., 2008). The most negative values of $\delta^{13}C$ correspond to the period 1700–
333 1500 AD (LIA) and are accompanied by high C_{org}/N values. Both factors
334 indicate the maximum terrestrial contribution during this period. In contrast, the

335 section at 94 cm depth (100–200 AD) had the second most positive $\delta^{13}C$ value
336 of the entire core and a low C_{org}/N ratio, matching with the numerous references
337 to a highstand occurring between 0 and 500 AD, equivalent to the Dunquerkian
338 transgression in northern Europe (Vilas et al., 1991; Devoy et al., 1996; Granja
339 et al., 1996; Martínez Cortizas et al., 1996) affecting Roman settlements
340 (Martínez Cortizas and Costa Casais, 1997; E5; Fig. 2). Other notable $\delta^{13}C$
341 oscillations downcore may indicate temporal changes in the source of OM or
342 climatic alterations (1100 or 700 AD), but modifications caused by
343 decomposition also have to be considered..

344 The core sections had extractable lipid content between 5.2 % and 16.9
345 % of the TOC (Fig. 2). A significant inverse correlation was observed between
346 lipid content (%TOC) and $\delta^{13}C$ value of TOC from 50 to 0 cm (1300–2010 AD; *r*
347 –0.73), suggesting a greater presence of land derived lipid material in the
348 extracts of the upper sections. Because of the significant increase in lipid
349 content for samples corresponding to 1100 and 500 AD (60 and 80 cm
350 respectively), the correlation disappeared in the lowest sections. This result may
351 indicate that environmental conditions enhanced lipid preservation or that
352 punctuated increases occurred in the lipid content of the sedimentary OM due
353 to fast flooding events (E3 and E4 in Fig. 2). The lipid content did not co-vary
354 with the carbonate content. In fact, yhe low pH and Ca content of Minho
355 estuarine water and marsh sediment interstitial water, resulting from the
356 absence of continental input of carbonate, prevent the development of
357 carbonated fauna in the marsh sediment, including calcareous benthic
358 foraminifera (Moreno et al., 2007; Fatela et al., 2009). Acidification in some

359 deep parts of the core increased the poor conservation of carbonate, i.e.
360 preventing the presence of macrofauna (González-Vila et al., 2003).
361
362 *4.2. Lipid biomarker distributions*
363 Fig. 3 shows SIM traces corresponding to *n*-alkanes (*m/z* 57), *n*-fatty
364 acids (FAs; *m/z* 74) and *n*-alkan-2-ones (*m/z* 58) in the uppermost section of the
365 core. These alkyl series have been widely used as part of geochemical proxies
366 for palaeoenvironmental reconstruction (Meyers and Ishiwatari, 1993).
367
368 *4.2.1. n-alkanes*
369 The *n*-alkane distribution was quite similar through the core, occur in the
370 C_{15}–C_{34} range (Fig. 3a) with a monomodal distribution maximising at C_{31} or C_{29}
371 and an odd predominance, which is usually related to the input of wax lipids
372 from higher plants. Several parameters using *n*-alkane abundance were used to
373 reconstruct changes in the origin of the sedimentary OM, vegetation type and
374 climate (Fig 4a). A common one is the carbon preference index (CPI), which is
375 used as indication of *n*-alkane source. A value ≥ 5 characterizes hydrocarbons
376 from vascular land plants, whereas values close to 1 are thought to indicate
377 greater input from marine microorganisms, petrogenic input and/or recycled OM
378 (Kennicutt et al., 1987). In environmental organic geochemistry, CPI is used to
379 indicate the degree of diagenesis of straight chain geolipids and is a numerical
380 representation of how much of the original biological chain length specificity is
381 preserved in geological lipids (Meyers and Ishiwatari, 1995). CPI values > 3;
382 Fig. 4a) indicated a clear odd/even predominance along the core, confirming a

greater terrestrial OM input. Samples corresponding to 1960–1985 and 100–200 AD had the lowest $^{o/e}$ values (2.4 and 2.8 respectively), suggesting a greater presence of marine phytoplankton, which may be related to the recent construction of dams and the marine highstand that occurred at these times (E1 and E5; Fig 2). Higher values were observed during the LIA, consistent with the increase in continental precipitation and reduced degradation during a cooler period (Xie et al., 2004). Another parameter is the average chain length of *n*-alkanes (ACL_{al}). Vegetation types is the main influence on the chain length of terrigenous leaf lipids (Poynter and Eglinton, 1990). Leaf lipids derived from grasslands have on average longer chain length than leaf lipids from plants in forests (Cranwell, 1973). The ACL values of C_{27}–C_{33} homologues (Bray and Evans, 1961) varied between 29.6 and 30.4 (avg., 30.1; Fig. 4a). Both the CPI and ACL oscillated during the end of the LIA, probably indicative of the above mentioned changing conditions (E2). They reached a maximum during the LIA, particularly during the Maunder minimum 1600–1700 AD which, according to previous studies, points to higher grass contribution (Juan et al., 2008). Typically, grass and herbs have ahigh concentration of C_{31} *n*-alkane, while trees, especially pines, are rich in C_{29}, but also show an important content of C_{27}. Therefore, the ratio C_{31}/C_{27} can be a proxy for reflecting shifts in vegetation from an open grass-dominated system to trees and forest landscape (Cranwell, 1973; Meyers and Ishiwatari, 1993). The C_{31}/C_{27} values in Fig. 4a indicate a progressive reduction in the forest area during the RWP, probably produced by changes in land use that occurred then (deforestation and intensification of cultivation), which is consistent with the progressive increase in ACL_{al} and

407 $CPI^{o/e}$. A sharp increase in grass contribution during the LIA (max. C_{31}/C_{27})
408 confirmed the outcome from $CPI^{o/e}$ and ACL_{al}. The terrigenous/aquatic ratio of
409 *n*-alkanes (TAR_{al}) is valuable for determining changes in relative contributions of
410 OM from land and aquatic flora although it may over-represent the absolute
411 amount from terrigenous sources (Meyers, 1997). The values ranged (Fig. 4a)
412 from 3.8 (1960–1985 AD) to 15.1(1600–1700 AD), which again pointed to a
413 significant reduction in continental discharge during the 1960s and 1970s (E1),
414 locating the maximum terrestrial signature during the LIA (Fig. 2). In addition,
415 the relative increase in TAR_{al} around 1100 AD is contemporaneous with large
416 magnitude floods reported for the Minho River in the course of the early MWP
417 (Benito et al., 1996; Abrantes et al., 2011; E3 in Fig 2).
418
419 *4.2.2. FAs*
420 The FAs ranged from C_{14}–C_{32} with a strong even predominance ($CPI^{e/o}$
421 3.1 to 6.1) and C_{max} at C_{26} (Figs. 3b, 4b). In addition, the monounsaturated FAs
422 ascribed to marine sources including bacteria and diatoms (Volkman et al.,
423 1980; Kruge and Permanyer, 2004) were scarce. It is well known that FAs are
424 more sensitive to degradation and modification than most types of biogenic
425 lipids and some are more susceptible to diagenesis than others; comparison
426 between different components can therefore help distinguish diagenetic effects
427 from source changes. Whereas the distributions in algae and bacteria maximize
428 at shorter chain length (C_{12}–C_{18}; Cranwell et al., 1987), C_{16} acids in particular
429 have been reported as ubiquitous in the biosphere, being found in land plants,
430 algae, bacteria and other microorganisms (Meyers, 1997). Longer chain (C_{22}–

431 C_{30}) homologues, present in all the samples, might be related to the waxy
432 coating of land plant-derived sources (Almendros et al., 1996), flowers and
433 pollen (Meyers and Ishiwatari, 1993). Parameters derived from the distribution
434 of FAs were consistent with the *n*-alkane behaviour. Maxima corresponding to
435 the $CPI^{e/o}$, ACL_{fa} (C_{24}–C_{30}) and TAR_{fa} for the LIA and around 1100 AD (early
436 MWP; E3), contrasted with the reduced values for 1960–1985 AD and 200–400
437 AD (Fig. 4b). The progressive increase through the RWP could be related to
438 deforestation and the intensification of human impact during that period.
439
440 *4.2.3. n-Alkan-2-ones*
441 A homologous series of *n*-alkan-2-ones (methyl ketones) from C_{15} to C_{31}
442 was detected in all the sections (Fig. 3c) The *n*-and exhibited a strong odd
443 predominance ($CPI^{o/e}_{ket}$ 2.9–4.4; Fig. 4c) with a maximum at C_{27}. The ACL
444 values for the C_{25}–C_{35} *n*-alkan-2-ones ranged from 27.0 to 27.9 (Fig. 4c). A
445 similar distribution has been reported to occur in many sedimentary
446 environments, including marine and lacustrine sediments (Volkman et al., 1983;
447 Meyers and Ishiwatari, 1993), soils, glacier ice and palaeosols (Xie et al., 2003),
448 and aerosols (Abas and Simoneit, 1996). Methyl ketones are usually formed by
449 microbially mediated α-oxidation of *n*-alkanes (Cranwell et al., 1987) or β-
450 oxidation and decarboxylation of *n*-FAs (Volkman et al., 1983), but have also
451 been reported to occur in higher plants, microalgae and phytoplankton
452 (Hernandez et al., 2001). For example, those maximizing at C_{27} are typical for
453 several *Juncus* species (Ortiz et al., 2011) growing in the study area,
454 suggesting a direct biological input from higher plants. The ACL and CPI values

displayed trends somewhat similar to the same parameters for *n*-alkanes and FAs throughout the sequence from the present until the early MWP. However, the opposite trend was observed for samples corresponding to the start of the MWP and the RWP. This could suggest a change in the dominant source of *n*-alkan-2-ones, such as the microbial oxidation of *n*-alkanes. The ratio $C_{25}/C_{27\ ket}$ has been used as an indicator of a marine contribution, the higher the value the greater the marine contribution (Hernández et al., 2001). Overall low C_{25}/C_{27ket} values (<1) were observed through the core (Fig. 4c), consistent with a strong terrigenous influence. Sections at 1960–1985 and 100–200 AD showed higher values of the C_{25}/C_{27ket}, in good agreement with $\delta^{13}C$, C_{org}/N and $CPI^{o/e}$al data (Figs. 2 and 4a), indicating a greater marine vs. planktonic input during these periods (E1 and E5; Fig. 2).

.

5. Conclusions

This study provides a comprehensive set of bulk geochemical indicators in combination with geochronology analysis and lipid assemblage to evaluate the changes in the predominant OM sources in a 1m core from the Minho tidal marsh. Radiocarbon dating revealed that the sediment sequence spans the past ca. 2000 yr. Sedimentation rate varied from ca. 0.5 to 1 mm yr^{-1} reflecting the regional trend for this type of environment.

The main conclusions can be summarized as:

(i) $\delta^{13}C$, TOC, TN, C/N and the distribution of *n*-alkyl biomarkers show that the OM in the core is primarily derived from terrestrial sources, reaching a maximum terrestrial signature during the Little Ice Age.

$C_{31}/C_{27al,}$ $CPI^{o/e}$ and ACL_{al} parameters indicate that grass vegetation dominated during this period.

(ii) Samples corresponding to the period 1960–1985 show low C_{org}/N ratio and heavier $\delta^{13}C$ values, as well as low CPI, ACL and TAR parameters, indicating a significant increase in marine input. This is likely due to the drastic reduction in the Minho River discharge associated with the construction of several major dams.

(1) (iii) Alternation in the C_{org}/N and $\delta^{13}C$ values through the 18^{th} and 19^{th} centuries is consistent with fluctuations in the *n*-alkyl parameters. They reveal common intensive precipitation alternating with severe droughts.

(2) (iv) High C_{org}/N, lipid content, ACL and TAR values at ca. 1100 AD suggest punctuated increases in the continental discharges, which is contemporaneous with major flood events reported for that period in the area.

(3) (v) The progressive increase in C_{31}/C_{27}, TAR_{al} and ACL_{al} values during the Roman Warm Period are probably produced by changes in land use practices that occurred at these times (deforestation and intensification of cultivation). High TS and very low C_{org}/S values could be derived from the mining exploitation during the Roman domination.

(4) (vi) Low C_{org}/N, $CPI^{o/e}$ and high $C_{25}/C_{27\ ket}$ values suggest a significant increase in the contribution of marine phytoplankton at 100–200 AD,

which may be related to the marine highstand during the early Roman Warm Period, as reported by several authors.

Acknowledgements

We acknowledge the funding by the Foundation for Science and Technology (FCT) of Portugal for J.M. M's PhD. Grant (SFRH/BD/45528/2008) and for the WestLog Project (PTDC/CTE-GIX/105370/2008). E.L. was awarded a Ralph E. Powe Junior Faculty Enhancement Award. This is a contribution to the IGCP Project 588 and to the Geo-Q Research Unit (Aranzadi). We would also like to thank Y. Xu and P.A. Meyers their careful reviewr and the valuable comments.

Guest Associate Editor – **V. Grossi**

References

Abas, M., Simoneit, B. R. T., 1996. Composition of extractable organic matter of air particles from Malaysia: An initial study. Atmospheric Environment 30, 2779–2793.

Abrantes, F., Rodrigues, T., Montanari, B., Santos, C., Witt, L., Lopes, C., Voelker, A.H.L. 2011. Climate of the last millennium at the southern pole of the North Atlantic Oscillation: an inner-shelf sediment record of flooding and upwelling. Climate Research 48, 261–280.

Alberts, J.J., Filip, Z., 1989. Sources and characteristics of fulvic and humic acids from a salt marsh estuary. The Science of the Total Environment 81–82, 353–361.

Almendros, G., Sanz, J., Velasco, F., 1996. Signatures of lipid assemblages in soils under continental Mediterranean forest. European Journal of Soil Science 47, 183–196.

Appleby, P.G., Oldfield, F., 1978. The calculation of lead-210 dates assuming a constant rate of supply of unsupported ^{210}Pb to the sediment. Catena 5, 1–8.

527 Appleby, P.G., Oldfield, F., 1992. Application of ^{210}Pb to sedimentation studies, In:
528 Ivanovich, M., Harmon, R.S. (Eds.), Uranium Series Disequilibrium. Oxford
529 University Press, Oxford, pp. 731–778.
530 Benito, G., Machado, M.J., Pérez-González, A., 1996. Climate change and flood
531 sensitivity in Spain. In: Branson, J., Brown, A.G., Gregory, K.J. (Eds.), Global
532 Continental Changes: The Context of Palaeohydrology. Geological Society Special
533 Publication 115, 95–98.
534 Benito, G., Thorndycraft V.R., Rico, M.,, Sánchez-Moya, Y., Sopeña, A., 2008
535 Palaeoflood and floodplain records from Spain: Evidence for long-term climate
536 variability and environmental changes. Geomorphology 101, 68–77.
537 Berner, R.A., 1989. Biogeochemical cycles of carbon and sulfur and their effect on
538 atmospheric oxygen over Phanerozoic time: Palaeogeography, Palaeoclimatology,
539 Palaeoecology 73, 97–122.
540 Bettencourt, A., Ramos, L., Gomes, V., Dias, J.M.A., Ferreira, G., Silva, M., Costa, L.,
541 2003. Estuários Portugueses. Ed. INAG – Ministério das Cidades, Ordenamento
542 do Território e Ambiente. Lisboa. 311 pp.
543 Bray, E.E., Evans, E.D., 1961. Distribution of *n*-paraffins as a clue to recognition of
544 source beds. Geochimica et Cosmochimica Acta 22, 2–15.
545 Burdloff, D., Araújo, M.F. Jouanneau, J.M., Mendes, I., Monge Soares, A.M., Dias,
546 J.M.A., 2008. Sources of organic carbon in the Portuguese continental shelf
547 sediments during the Holocene period. Applied Geochemistry 23, 2857–2870.
548 Cranwell, P.A., 1973. Chain-length distribution of *n*-alkanes from lake sediments in
549 relation to post-glacial environmental change. Freshwater Biology 3, 259–265.
550 Cranwell, P.A., Eglinton, G., Robinson, N., 1987. Lipids of aquatic organisms as
551 potential contributors to lacustrine sediments–II. Organic Geochemistry 11, 513–
552 527.

553 Cundy, A.B., Croudace, I.W., 1995. Sedimentary and geochemical variations in a salt-
554 marsh mud flat environment from the mesotidal Hamble estuary, southern
555 England. Marine Chemistry 51, 115-132.
556 De La Rosa Arranz, J.M.; González-Pérez, J.A. González-Vila, F.J., Knicker, H.,
557 Araújo, F., 2011. Molecular composition of sedimentary humic acids from South
558 West Iberian Peninsula: A multiproxy approach. Organic Geochemistry 42, 791–
559 802.
560 Desprat, S., Goñi, M.F.S. and Loutre, M.-F. 2003. Revealing climatic variability of the
561 last three millennia in northwestern Iberia using pollen influx data. Earth and
562 Planetary Science Letters 213, 63–78.
563 Devoy, R.J.N., Delaney, C., Carter, R.W.G., Jennings, S.C., 1996. Coastal
564 stratigraphies as indicators of environmental changes upon European Atlantic
565 coast in the late holocene. Journal of Coastal Research 12, 564–588.
566 Fatela, F., Moreno, J., Moreno, F., Araújo, M.F., Valente, T., Antunes, C., Taborda, R.,
567 Andrade, C., Drago, T., 2009. Environmental constraints of foraminiferal
568 assemblages distribution across a brackish tidal marsh (Caminha, NW Portugal).
569 Marine Micropaleontology 70, 70–88.
570 Ficken, K. J., Wooller, M. J., Swain, D. L., Street-Perrott, F. A., Eglinton, G., 2002.
571 Reconstruction of a subalpine grass-dominated ecosystem, Lake Rutundu, Mount
572 Kenya: a novel multi-proxy approach, Palaeogeography, Palaeoclimatology,
573 Palaeoecology 177, 137–149.
574 Flynn, W.W., 1968. Determination of low levels of ^{210}Po in environmental materials.
575 Analytica Chimica Acta 43, 221–227.
576 Gil-Garcia, M.J., Ruiz Zapata, M.B., Mediavilla, R, Santisteban, J.I., Dominguez-
577 Castro, F., Dabrio, C.J., 2008. Registro de los cambios humanos y naturales en el
578 humedal de las Tablas de Daimiel (Ciudad Real, España). Geo-Temas 10, 1471–
579 1474.

González-Vila, F.J., Polvillo, O., Boski, T., Moura, D., de Andrés, J.R., 2003. Biomarker patterns in a time-resolved Holocene/terminal Pleistocene sedimentary sequence from the Guadiana river estuarine area (SW Portugal/Spain border). Organic Geochemistry 34, 1601–1613.

Granja, E.M., Thomas, A.M., De Groot, 1996. Sea-level rise and neotectonism in a Holocene coastal environment at Cortegaça beach (NW Portugal): a case study. Journal of Coastal Research12, 160–170.

Hadas, O., Pinkas, R., Malinsky-Rushansky, N., Markel, D., Lazar, B., 2001. Sulfate-reduction in lake Agmon, Israel. Science of the Total Environment 266, 202–209.

Hashimoto, N., Adyama, T., Shioiri, T., 1981. New methods and reagentsin organic synthesis. A simple efficient preparation of methyl esters with trimethylsilydiazomethane (TMSCHN2) and its application to gas chromatographic analysis of fatty acids. Chemical & Pharmaceutical Bulletin 29,1475–1478.

Hedges, J.I., Oades, J.M., 1997. Comparative organic geochemistry of soils and marine sediments, Organic Geochemistry 27, 319–361.

Hernández, M.E., Mead, R., Peralba, G., Jaffé, R., 2001. Origin and transport of *n*-alkan-2-ones in a subtropical estuary: potential biomarkers for seagrass-derived organic matter. Organic Geochemistry 32, 21–32.

Holtvoeth, K., van Griensven, A., Seuntjens, P., Vanrolleghem, P.A., 2005. Sensitivity analysis for hydrology and pesticide supply towards the river in SWAT. Physics and Chemistry of the Earth 30, 518–526.

Irabien, M.J., Cearreta, A., Leorri, E., Gomez, J., Viguri, J., 2008. A 130 year record of pollution in the Suances estuary (southern Bay of Biscay): Implications for environmental management. Marine Pollution Bulletin 56, 1719–1727.

Juan, H., MeiXun, Z., Li, L., PinXian, W., HuangMin, G., 2008. Sea surface temperature and terrestrial biomarker records of the last 260 ka of core MD05-

2904 from the northern South China Sea. Chinese Science Bulletin 53, 2376–2384.

Kennicutt, M. C., Barker, C., Brooks, J. M., DeFreitas, D.A., Zhu, G.H., 1987. Selected organic matter source indicators in the Orinoco, Nile, and Changjiang Deltas. Organic Geochemistry 11, 41–51.

Kruge, M.A., Permanyer, A., 2004. Application of pyrolysis-GC/MS for rapid assessment of organic contamination in sediments from Barcelona harbour. Organic Geochemistry 35, 1395–1408.

Lamb, A.L., Wilson, G.P., Leng, M. J., 2006. A review of coastal palaeoclimate and relative sea-level reconstructions using $\delta^{13}C$ and C/N ratios in organic material. Earth-Science Reviews 75, 29–57.

Lehmann, M.F., Bernasconi, S.M., Barbieri, A., McKenzie, J.A., 2002. Preservation of organic matter and alteration of its carbon and nitrogen isotope composition during simulated and in situ early sedimentary diagenesis. Geochimica et Cosmochimica Acta 66, 3573–3584.

Leorri, E., Horton B.P., Cearreta, A., 2008. Development of a foraminifera-based transfer function in the Basque marshes, N. Spain: Implications for sea-level studies in the Bay of Biscay. Marine Geology 251, 60–74.

Leorri, E., Cearreta, A., Corbett, R., Blake, W., Fatela, F., Gehrels, R., Irabien, M.J., 2010. Identification of suitable areas for high-resolution sea-level studies in SW Europe using commonly applied ^{210}Pb models. Geogaceta 48, 35–38.

Leventhal, J., 1983. Interpretation of C and S relationships in Black Sea sediments. Geochimica et Cosmochimica Acta 47, 133–137.

Martin-Puertas, C., Valero-Garces, B.L., Mata, M.P., Gonzalez-Samperiz, P., Bao, R., Moreno, A., Stefanova, V., 2008. Arid and humid phases in Southern Spain during the last 4000 years: the Zonar Lake record, Cordoba. The Holocene 18, 1–15.

632 Martínez Cortizas, A., Costa Casais, M., 1997. Indicios de variaciones del nivel del mar
633 en la ría de Vigo durante los últimos 3000 años. Gallaecia 16, 23–47.
634 Martínez Cortizas, A., Costa Casais, M., Moares Dominguez, C., 1996. Niveles
635 dunares pleistocenos y holocenos en la costa de Galicia: hipótesis cronológica en
636 base a su grado de edafización. In: Pérez Alberti, A., Martini, P., Chesworth, W.,
637 Martínez Cortizas, A. (Eds.), Dinámica y Evolución de Medios Cuaternarios. Xunta
638 de Galicia, Santiago, pp. 391–404.
639 Martínez Cortizas, A., Pontevedra-Pombal, X., Garcia-Rodeja, E., Novoa-Muñoz, J.C.
640 and Shotyk, W. 1999. Mercury in a Spanish peat bog: Archive of climate change
641 and atmospheric metal deposition. Science 284, 939–942.
642 Meyers, P.A., Leenheer, M.J., Eadie, B.J., Maule, S.J., 1984. Organic geochemistry of
643 suspended and settling particulate matter in Lake Michigan. Geochimica. et
644 Cosmochimica Acta 48, 443–452.
645 Meyers, P.A., 1994. Preservation of elemental and isotopic source identification of
646 sedimentary organic matter. Chemical Geology 144, 289–302.
647 Meyers, P.A., 1997. Organic geochemical proxies of paleoceanographic,
648 paleolimnologic and paleoclimatic processes. Organic Geochemistry 27, 213–250.
649 Meyers, P.A., Ishiwatari, R., 1993. Lacustrine organic geochemistry – an overview of
650 indicators of organic matter sources and diagenesis in lake sediments. Organic
651 Geochemistry 20, 867–900.
652 Meyers, P.A., 2003. Applications of organic geochemistry to paleolimnological
653 reconstructions: a summary of examples from the Laurentian Great Lakes.
654 Organic Geochemistry 34, 261–289.
655 Moreno, J., Valente, T., Moreno, F., Fatela, F., Guise, L., Patinha, C., 2007.
656 Occurrence of calcareous foraminifera and calcite equilibrium conditions – a case
657 study in Minho/Coura estuary (Northern Portugal). Hydrobiologia 587, 177–184.

658 Müller, A., Mathesius, U., 1999. The palaeoenvironments of coastal lagoons in the
659 southern Baltic Sea, I. The application of sedimentary Corg/N ratios as source
660 indicators of organic matter. Palaeogeography, Palaeoclimatology, Palaeoecology
661 145, 1–16.
662 Nieuwenhuize, J., Maas, Y.E., Middelburg, J., 1994. Rapid analysis of organic carbon
663 and nitrogen in particulate materials. Marine Chemistry 45, 217–224.
664 Nittrouer, C.A., Sternberg, R.W., Carpenter, R., Bennett, J.T., 1979. The use of ^{210}Pb
665 geochronology as a sedimentological tool: application to the Washington
666 Continental Shelf. Marine Geology. 297–316.
667 Ortiz, J.E., Díaz-Bautista, A., Aldasoro, J.J., Torres, T., Gallego, J.L.R., Moreno, L.,
668 Estébanez, B., 2011. n-Alkan-2-ones in peat-forming plants from the Roñanzas
669 ombrotrophic bog (Asturias, northern Spain). Organic Geochemistry 42, 586–592.
670 Perdue, E.M., Koprivnjak, J.F., 2007. Using the C/N ratio to estimate terrigenous inputs
671 of organic matter to aquatic environments. Estuarine, Coastal and Shelf Science
672 74, 65–72.
673 Pla, S., Catalan, J., 2005. Chrysophyte cysts from lake sediments reveal the
674 submillennial winter/spring climate variability in the northwestern Mediterranean
675 region throughout the Holocene. Climate Dynamics 24, 263–278.
676 Polvillo, O., González-Pérez, J., Boski, T., González-Vila, F.J., 2009. Structural
677 features of humic acids from a sedimentary sequence in the Guadiana estuary
678 (Portugal-Spain border). Organic Geochemistry 40, 20–28.
679 Poynter, G., Eglinton, G., 1990. Molecular composition of three sediments from hole
680 717C: The Bengal Fan. In: Cochran, J.R., Stow, D.A.V. et al. (Eds.), Proceedings
681 of the Ocean Drilling Program, Scientific Results 116, pp. 155–161.
682 Prahl F., Ertel J., Goni M., Sparrow M., Eversmeyer B., 1994. Terrestrial organic
683 carbon contributions to sediments the Washington margin. Geochimica et
684 Cosmochimica Acta 58, 3035–3048.

685 Reimer, P.J., Baillie, M.G.L., Bard, E., Bayliss, A., Beck, J.W., Blackwell, P.G., Bronk
686 Ramsey, C., Buck, C.E., Burr, G.S., Edwards, R.L., Friedrich, M., Grootes, P.M.,
687 Guilderson, T.P., Hajdas, I., Heaton, T.J., Hogg, A.G., Hughen, K.A., Kaiser, K.F.,
688 Kromer, B., McCormac, G., Manning, S., Reimer, R.W., Richards, D.A., Southon,
689 J.R., Talamo, S., Turney, C.S.M., van der Plicht, J., Wehenmeyer, C.E., 2009.
690 IntCal09 and Marine09 Radiocarbon Age Calibration Curves, 0-50,000 Years cal
691 BP. Radiocarbon 51, 1111–1150.
692 Riera, S., Wansard, G., Juliá, R., 2004. 2000-Year environmental history of a karstic
693 lake in the Mediterranean Pre-Pyrenees: the Estanya lakes (Spain). Catena 55,
694 293–324.
695 Robbins, J.A., 1978. Geochemical and geophysical applications of radioactive lead, In:
696 Nriagu, J.O. (Ed.), The Biogeochemistry of Lead in the Environment, Publisher?,
697 pp. 285–377.
698 Rosell Melé, A., 2003. Biomarkers as proxies of climate change. In: Mackay, A.,
699 Battarbee, R.W., Birks, J., Oldfield, F., (Eds.), Global changes in the Holocene.
700 Arnold, London, pp. 358–372.
701 Sabel, M., Bechtel, A., Püttmann, W., Hoernes, S., 2005. Palaeoenvironment of the
702 Eocene Eckfeld Maar lake (Germany): implications from geochemical analysis of
703 the oil shale sequence. Organic Geochemistry 36, 873–891.
704 Sánchez-Palencia, F.J., Suárez, V., 1988. La mineríaa antigua del oro en Asturias. In:
705 Hunosa, X. (Ed.), Libro de la Mina. Asturias, pp. 221–242.
706 Schmidt, F., Hinrichs, K.-U., Elvert, M., 2010. Sources, transport and partitioning of
707 organic matter at a highly dynamic continental margin. Marine Chemistry 118,
708 37–55.
709 Schmidt, F., Elvert, M., Koch, B.P., Witt, M., Hinrichs, K-U., 2009. Molecular
710 characterization of dissolved organic matter in pore water of continental shelf
711 sediments. Geochimica et Cosmochimica Acta 73, 3337–3358.

712 Thornton, S. F., McManus, J., 1994. Application of organic Carbon and Nitrogen stable
713 isotope and C/N ratios as source indicators of organic matter provenance in
714 estuarine systems: evidence from the Tay Estuary, Scotland. Estuarine, Coastal
715 and Shelf Science 38, 219–233.
716 Uzaki M., Ishiwatari R., 1986. Carbohydrates in the sediment of lake Yunoko: vertical
717 distribution and implication to their origin. Japan Journal of Limnology 47, 257–
718 267.
719 Vilas, F., Sopeña, A., Rey, L., Ramos, A., Nombela, M.A., Arche, A., 1991. The
720 Corrubedo beach-lagoon complex, Galicia, Spain:dynamics, sediments and recent
721 evolution of a mesotidal coastalembayment. Marine Geology 97, 391–404.
722 Volkman, J.K., Johns, R.B., Gillan, F.T., Perry, G.J., Bavor Jr., H.J., 1980. Microbial
723 lipids of an intertidal sediment-I. Fatty acids and hydrocarbons. Geochimica et
724 Cosmochimica Acta 44, 1133–1143.
725 Volkman, J.K., Farrington, J.W., Gagosian, R.B., Wakeham, S.G., 1983. Lipid
726 composition of coastal sediments from the Peru upwelling region. In: Bjoroy, M., et
727 al.(Eds.), Advances in Organic Geochemistry 1981.Wiley, Chichester, pp. 28–240.
728 Volkman, J.K., 2006. Lipid markers for marine organic matter. In: Volkman, J.K. (Ed.),
729 Handbook of Environmental Chemistry: Reactions and Processes vol. 2, Springer,
730 Berlin. pp. 27–70.
731 Wakeham, S.G., Beier, J.A., Clifford, C.H., 1991. Organic matter sources in the Black
732 Sea as inferred from hydrocarbon distributions. In: Izdar, E., Murray, J.W., 1991.
733 (Eds.), Black Sea Oceanography, Kluwer Academic, The Netherlands, pp. 319–
734 341.
735 Xie, S., Nott, C.J., Avsejs, L.A, Maddy, D., Chambers, F.M., Evershed, R.P., 2004.
736 Molecular and isotopic stratigraphy in an ombrotropic mire for palaeoclimate
737 reconstruction. Geochimica et Cosmochimica Acta 68, 2849–2862.
738

Figure captions

Fig. 1. Location of study area. Dark grey area, Caminha tidal marsh. C, core location (CP W1).

Fig. 2. Downcore plots of geochronology and bulk characteristics.. E 1, damp and dry period; E 2, dry-flood events; E 3 and E 4, floods; E 5, marine highstand.

Fig. 3. Reconstructed ion chromatograms of (a) n-alkanes (*m/z* 57), (b) *n*-FA methyl esters (*m/z* 74) and (c) *n*-alkan-2-ones (*m/z* 58) in 0–2 cm section of core. Numbers on peaks refer to chain length.

Fig. 4. Parameters from *n*-alkyl compounds. $CPI^{o/e}_{al}$, Carbon Preference Index = Σ area C odd/Σ area C even; ACL, average chain length; TAR_{al}, terrigenous to aquatic ratio of *n*-alkanes = (area C_{27} + C_{29} + C_{31})/(area C_{15} + C_{17} + C_{19}); $C_{31}/C_{27\ alk}$ = area C_{31}/area C_{27} of *n*-alkanes; $CPI^{e/o}$, Carbon Preference Index = Σ area C even / Σ area C odd; TAR_{fa}, terrigenous to aquatic ratio of *n*-FAs (C_{24} + C_{26} + C_{28})/(C_{12} + C_{14} + C_{16}); $C_{25}/C_{27\ ket}$ = area C_{25}/area C_{27} of *n*-alkan-2ones.

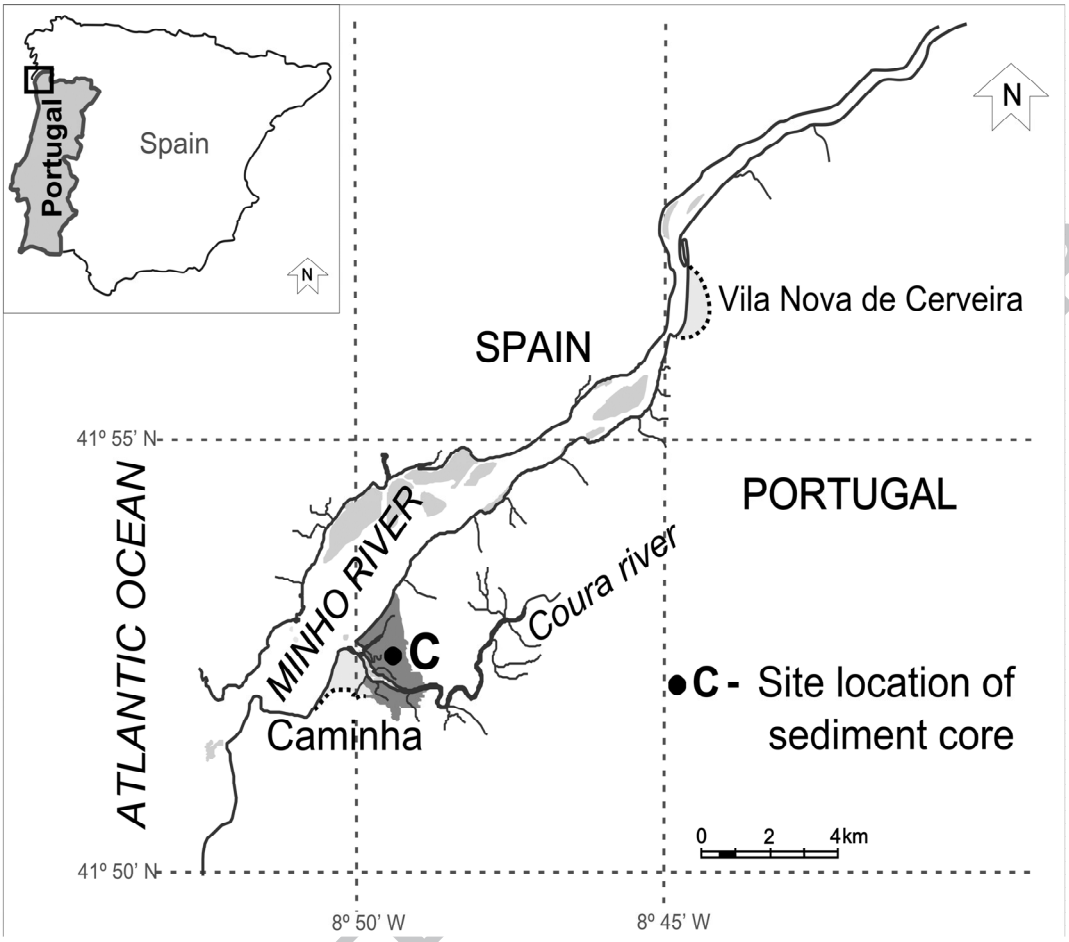

759

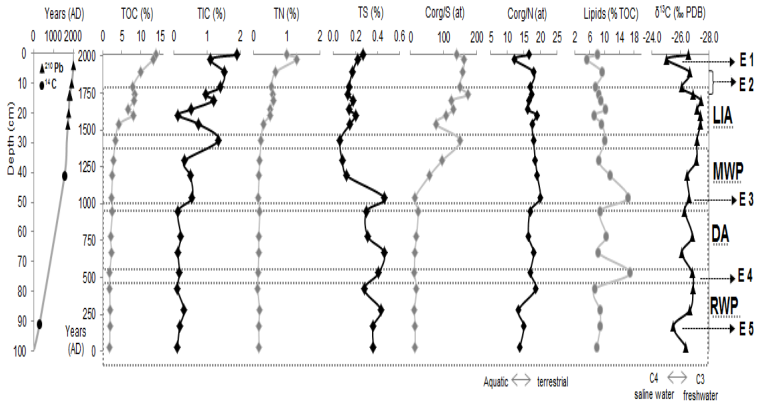

760

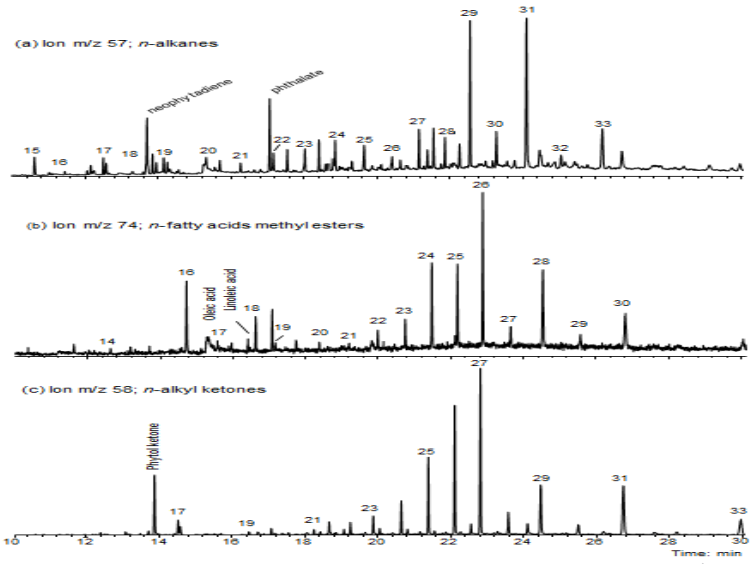

761

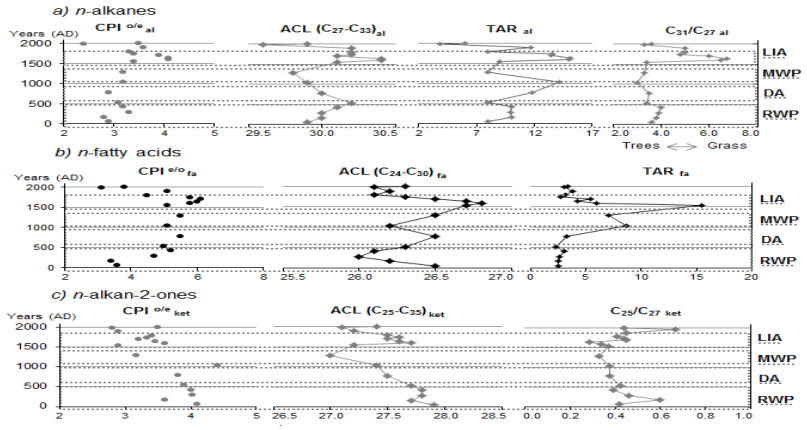

762

763
764 **Table 1**
765 Radiocarbon data.

Sample code	Laboratory code	Depth (cm)	Analysis	Conventional age	2 sigma calibration
CP 41	Beta-304385	41	AMS-Standard delivery	380 +/- 30 BP	Cal AD 1440 to 1530 / Cal AD 1560 to 1630
CP 91	Beta-304386	91	AMS-Standard delivery	1760 +/- 30 BP	Cal AD 220 to 350

766
767